

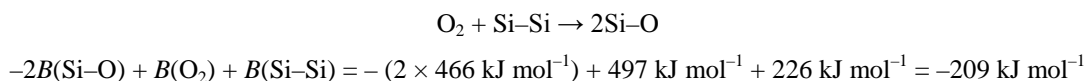
## Guidelines for Selected Tutorial Problems

### Chapter 1 Atomic Structure

- T1.2** Your coverage of early proposals for the periodic table should at least include Döbereiner's triads, Newlands' Law of Octaves, and Meyer's and Mendeleev's tables. From the modern designs (post-Mendeleev) you should consider Hinrichs' spiral periodic table, Benfey's oval table, Janet's left-step periodic table, and Dufour's Periodic Tree. A good starting reference for this exploration is Eric R. Scerri. (1998). The Evolution of the Periodic System. *Scientific American*, 279, 78–83 and references provided at the end of this article. The website "The Internet Database of Periodic Tables" ([http://www.meta-synthesis.com/webbook/35\\_pt/pt\\_database.php](http://www.meta-synthesis.com/webbook/35_pt/pt_database.php)) is also useful.
- T1.6** The variation of atomic radii is one of the periodic trends, and as such could be used to group the elements. Look up the atomic radii of the six elements and see which grouping, (a) or (b), better follows the expected trends in atomic radii. After that you should extend your discussion to the chemical properties of the elements in question and see if your choice makes chemical sense as well.

### Chapter 2 Molecular Structure and Bonding

- T2.2** The substances common in the Earth's crust are silicate minerals. These contain Si–O bonds with no Si–Si bonds. On the other hand, biosphere contains living systems that are based on biologically important organic molecules that contain C–C and C–H bonds. To understand this "segregation" of Si and C (both elements of the Group 14) we have to analyse the mean bond enthalpies,  $B$ , for these bonds listed in Table 2.8. If we concentrate on silicon first, we see that the bond enthalpy for Si–Si bond is about  $\frac{1}{2}$  of the Si–O bond ( $226 \text{ kJ mol}^{-1}$  vs.  $466 \text{ kJ mol}^{-1}$ ). Also, Si–H bond enthalpy is about  $\frac{2}{3}$  of Si–O bond ( $318 \text{ kJ mol}^{-1}$  vs.  $466 \text{ kJ mol}^{-1}$ ). Consequently, any Si–Si and Si–H bonds will be converted to Si–O bonds (and water in the case of Si–H). Although it appears that the bond enthalpy of  $\text{O}_2$  molecule is high ( $497 \text{ kJ mol}^{-1}$ ), keep in mind that two Si–O bonds are formed if we break one molecule of  $\text{O}_2$ . Thus, we are considering the following general reaction and associated changes in enthalpy:



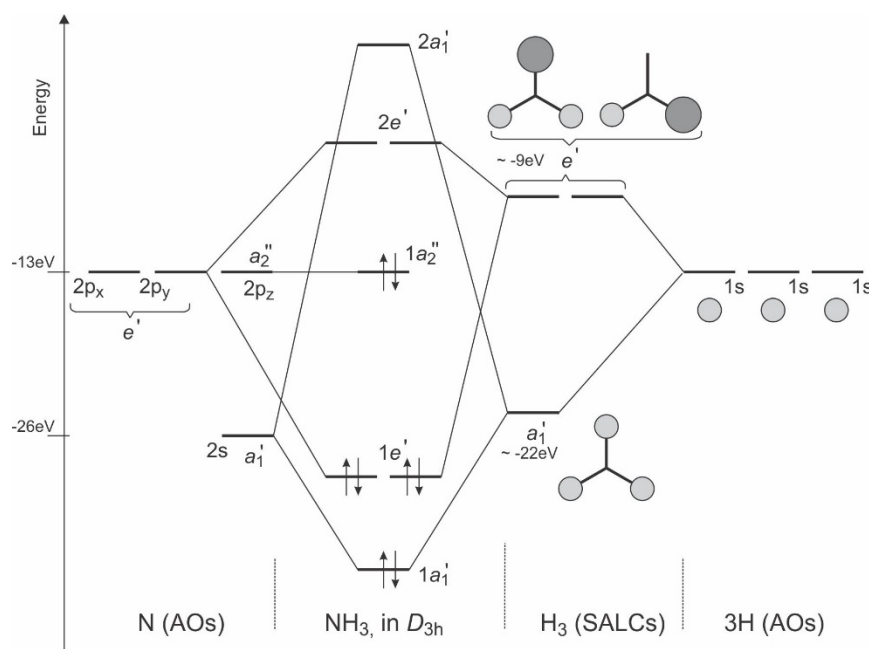
Positive signs above indicate that the energy has to be used (i.e., we have to use up the energy to break  $\text{O}=\text{O}$  and Si–Si bonds) while the negative sign indicates energy released upon a bond formation (i.e., energy liberated when Si–O bond is formed). As we can see, the process is very exothermic and as long as there is  $\text{O}_2$ , Si will be bonded to O rather than to another silicon atom. Very similar calculations can be performed to show the preference of Si–O bond over Si–H bond, but in this case formation of very strong H–O bonds (about  $463 \text{ kJ mol}^{-1}$  per H–O bond) has to be taken into account. This would result in even more exothermic process.

Carbon on the other hand, forms much stronger bonds with H and O in comparison to silicon. It also forms much stronger C–C double and triple bonds in comparison to Si–Si triple bonds. (Recall that as we descend a group the strength of  $\pi$  bonds decrease due to the increased atomic size and larger separation of p atomic orbitals in space. This larger separation prevents efficient orbital overlap.) You will note that the formation of C–O and O–H bonds from organic material (C–C bonds) is still somewhat exothermic, but a high bond enthalpy in  $\text{O}_2$  molecule presents a high activation barrier. Thus, we do need a small input of energy to get the reaction going—a spark to light a piece of paper or burning flame to light camp fire.

- T2.6** The planar form of  $\text{NH}_3$  molecule would have a trigonal planar molecular geometry with the lone pair residing in nitrogen's p orbital that is perpendicular to the plane of the molecule. This structure belongs to a  $D_{3h}$  point group (for discussion of molecular symmetry and point groups refer to Chapter 7). Now we can consult Resource Section 5. Table RS5.1 proves us with *the symmetry classes* of atomic orbitals on a central atom of  $\text{AB}_n$  molecules. In our case, the central atom is N with its 2s and 2p valence orbitals. From the table, we look at the symmetry classes of s and p orbitals (table rows) for the  $D_{3h}$  point group (in columns). We can see that the s orbital is in  $A_1'$  class (a non-degenerate orbital),  $p_x$  and  $p_y$  in  $E'$  class (a doubly degenerate orbital), and finally  $p_z$  is in  $A_2''$  class (again a single degenerate orbital).

Recall from Section 2.9(a) *Polyatomic molecular orbitals* that molecular orbitals are formed as linear combinations of atomic orbitals of the same symmetry and similar in energy. We find first a linear combination of atomic orbitals on peripheral atoms (in this case H) and the coefficient  $c$ , and then combine the combinations of appropriate symmetry with atomic orbitals on the central atom. The linear combinations of atomic orbitals of peripheral atoms (also called symmetry-adapted linear combinations—SALC) are given after Table RS5.1 in the Resource Section 5. Thus, we have to find linear combinations in  $D_{3h}$  point group that belong to symmetry classes  $A_1'$ ,  $A_2''$ , and  $E'$ . We also have to keep in mind that H atom has only one s orbital.

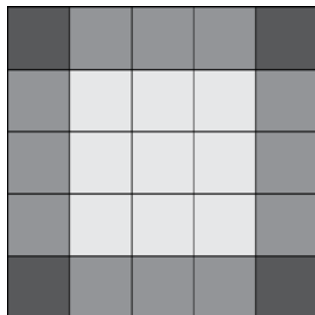
We can find one  $A_1'$  and two  $E'$  linear combinations that are based only on s orbitals (all other given combinations in the  $D_{3h}$  group with the same symmetry class are based on p orbitals—this can be concluded based on the orbital shape). This means that  $p_z$  atomic orbital on nitrogen atom (from  $A_2''$  class) does not have a symmetry match in the linear combinations of hydrogen's s orbitals and will remain essentially a non-bonding orbital in the planar  $NH_3$  molecule. The plot is given below. Keep in mind the relative energies of atomic orbitals given in the text of the problem. These are important because only orbitals of right symmetry and similar energies will combine to make molecular orbitals. Further note that  $A_1'$  linear combination of H atomic orbitals is lower in energy than  $E'$  combinations because there are no nodes in the case of  $A_1'$  combinations. (In the plot below AOs stands for “atomic orbitals” and SALC stands for “symmetry-adapted linear combinations.” Both H atomic orbitals and SALCs formed from them are sketched.)



## Chapter 3 The Structures of Simple Solids

**T3.2** Considering that fcc unit cell contains four atoms and given dimension of gold's unit cell, it is possible to calculate the number of Au atoms in the nanoparticle as follows

The unit cell length of 2000 nm represents 5 unit cells so the nanoparticle cube contains  $5 \times 5 \times 5 = 125$  unit cells. A low estimate for the number of atoms would use the number of atoms in a fcc unit cell in an infinite crystal (=4) giving  $4 \times 125 = 500$  gold atoms; however unlike an infinite crystal the gold atoms on the faces of the nanocube are not shared with neighbouring unit cells and contribute fully to the number of atoms in the cubic nanoparticle. There are various mathematical ways of tackling this problem but from a crystallographic point of view we can count atoms in the various unit cells that are internal, or on the surface of the nanocube, see the Figure that shows one face of the cube.



The  $5 \times 5 \times 5$  unit will have  $3 \times 3 \times 3 = 27$  unit cell unit embedded at the centre of the cube and these cells will be equivalent to those within an infinite crystal and therefore have 4 Au atoms per unit cell. The total number of atoms contributed to the nanoparticle is thus  $27 \times 4 = 108$  Au atoms. Consideration of a cube face shows there are nine unit cells that have one external surface, shaded pale grey in the Figure. Counting the number of gold atoms contributing to the gold nanoparticle in this type of cell gives  $(4 \times 1/8) + (5 \times 1/2) + (4 \times 1/4) + (1 \times 1) = 5$ ; there are 6 faces of the cube giving the total of  $6 \times 9 \times 5 = 270$ . For the cell shaded mid grey the calculation gives  $3(\text{unit cells per edge}) \times 12(\text{number of edges to nanocube}) \times 6.25(\text{number of atoms contributed by this type of unit cell}) = 225$ . Final for the corner units shaded dark grey the calculation is  $8 \times 7.875 = 63$ . The total number of atoms in the nanocube is thus  $108 + 270 + 225 + 63 = 666$  Au atoms.

For a general nanocube with  $n$  unit cells along each edge the number of atoms in the nanocube is given by

$$4m^3 - 6m^2 + 3m$$

Where  $m = n + 1$ , that is the number of atoms along the nanocube edge.

When considering the interaction with light, it is important to consider the wavelengths of the visible light and the size of nanoparticles.

**T3.4** The Madelung constant is in a sense a geometrical factor that depends on the position of ions within a unit cell. The electrostatic potential in which  $\text{Na}^+$  ions resides is given by:

$$V = \frac{z^2 e^2}{4\pi\epsilon_0 d}$$

where in this case  $d$  is the distance between  $\text{Na}^+$  and the neighbouring atoms we are considering. The first neighbours are 6  $\text{Cl}^-$  ions at the distance  $d$ . Thus, the potential energy of a single  $\text{Na}^+$  surrounded by six anions is:

$$V_1 = -\frac{6e^2}{4\pi\epsilon_0 d}$$

Next, we have 12  $\text{Na}^+$  ions (the ones located on the faces of the cubic unit cell). Using Pythagoras's theorem, we can show that they are at the distance of  $d\sqrt{2}$  from the same  $\text{Na}^+$  we looked at above (see Figure T3.2 below). This is a repulsive interaction for which we get the following potential  $V_2$ :

$$V_2 = +\frac{12e^2}{4\pi\epsilon_0 \sqrt{2}d}$$

Next to consider are eight  $\text{Cl}^-$  ions at the middle of each edge of the unit cell. Again, using Pythagoras's theorem we can see that the distance between them and our  $\text{Na}^+$  is  $d\sqrt{3}$ . The potential  $V_3$  is thus:

$$V_3 = -\frac{8e^2}{4\pi\epsilon_0 \sqrt{3}d}$$

This process can be continued in the same manner until  $V_6$ , which would give all six terms in the Madelung series given in this project (Figure P3.2 shows the distances involved in calculation of all  $V_n$ ).

To find the total potential for  $\text{Na}^+$  cation we have to sum  $V_1, V_2, V_3$ , etc.:

Weller, *Inorganic Chemistry* International Edition  
**Guidelines for Selected Tutorial Problems**

$$\begin{aligned}
 V_{tot} &= V_1 + V_2 + V_3 + \dots = \\
 &= -\frac{6e^2}{4\pi\epsilon_0 d} + \frac{12e^2}{4\pi\epsilon_0 d\sqrt{2}} - \frac{8e^2}{4\pi\epsilon_0 d\sqrt{3}} + \dots = \\
 &= -\frac{e^2}{4\pi\epsilon_0 d} \left( \frac{6}{\sqrt{1}} - \frac{12}{\sqrt{2}} + \frac{8}{\sqrt{3}} - \dots \right)
 \end{aligned}$$

The value of the series in the brackets is called the Madelung constant for NaCl type structure.

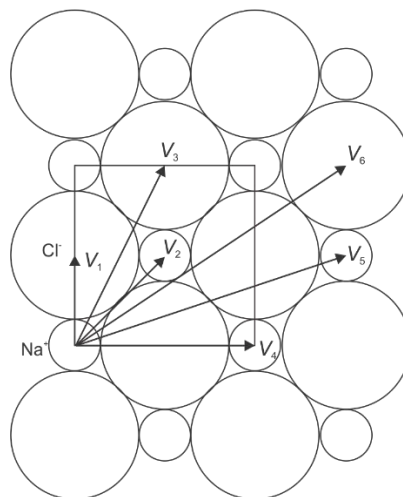


**Figure T3.2**

- T3.8** Note that for the case of MX salts the product of charges is 1 and  $N_{\text{ion}} = 2$ . The change from pm (in Kapustinskii's equation) to nm (in Bartlett's relationship) is responsible for change in the order of magnitude in the numerator. Also, the volume in Bartlett's relationship is the volume of the formula unit (simple NaCl) and not of the unit cell, and as such is directly proportional to the anion and cation radii in Kapustinskii's equation.

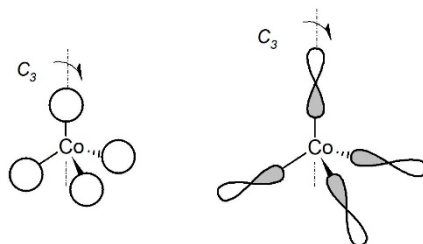
## Chapter 4 Molecular Symmetry

- T4.1** Use VSEPR theory to deduce the molecular geometry of  $\text{IF}_3\text{O}_2$ , then analyse all possible arrangement of F and O atoms around the central I atom that cannot be superimposed on each other (you should get three isomers). Follow the decision tree to determine the point group of each isomer.
- T4.3** The cation  $\text{NH}_4^+$  has a tetrahedral geometry and hence belongs to  $T_d$  point group. Looking at the character table we can see that we have to consider the degeneracy; for example,  $T_2$  has (x,y,z) in the last column. This means that the vibration is going to be active along all three axes and degeneracy should be expected.
- T4.5** From VSEPR,  $\text{AsCl}_5$  should be trigonal bipyramidal with symmetry  $D_{3h}$ . We first obtain the representation  $\Gamma_{3N}$ :

$D_{3h}$	$E$	$2C_3$	$3C_2$	$\sigma_h$	$2S_3$	$3\sigma_v$
$\Gamma_{3N}$	18	0	-2	4	-2	4

$\Gamma_{3N}$  reduces to:  $2A_1' + A_2' + 4E' + 3A_2'' + 2E''$ ; subtracting  $\Gamma_{\text{trans}} (E' + A_2'')$  and  $\Gamma_{\text{rot}} (A_2' + E'')$ , we obtain  $\Gamma_{\text{vib}} : 2A_1' + 3E' + 2A_2'' + E''$ . Thus we expect six Raman bands:  $2A_1' + 3E' + E''$  (note that  $A_2''$  is inactive in Raman because symmetry type does not contain the same symmetry as the function  $x^2 + y^2 + z^2$ ).

- T4.7** The easiest way to approach this tutorial problem is to sketch the Cl orbitals in tetrahedral arrangement around  $\text{Co}^{2+}$  as shown below (note that all p orbitals face the central metal cation with the same phase). Then, start applying the symmetry elements and see how each set of orbitals is behaving. The sketch shows the location of one of the four three-fold rotation axes, and rotation for  $120^\circ$  round this axis leaves all orbitals unchanged.



Keep in mind that both the orbital shape and the phases of individual lobes must match to claim that orbitals are unchanged. To show that indeed both sets of Cl orbitals transform in identical manner, all symmetry elements for the  $T_d$  point group must be checked.

For bonding, consider the symmetry requirements for orbital bonding and the possibility of p orbitals contribution to Co–Cl bonding.

- T4.9** Take a 3d transition metal as a central atom surrounded by six monoatomic ligands. First, assign the metal's 3d, 4s and 4p valence orbitals to a proper symmetry species using the first table in the Resource Section 5.

Now you have to construct SALCs that would have the same symmetry species as some metal orbitals. For the  $\sigma$  bonding use simple s atomic orbital. Your SALCs should look like the ones provided in the later part of Resource Section 5 under  $O_h$  point group.

For  $\pi$  bonding use p orbitals. Your final result is also given in Resource Section 5 for  $O_h$  point group.

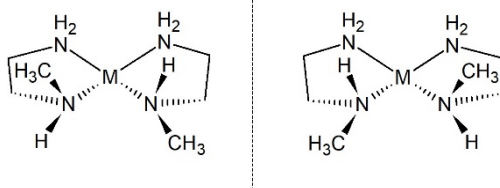
## Chapter 5 Acids and Bases

- T5.5** Start from Section 5.16 Superacids and superbases which covers “classical” examples of superbases, nitrides, and hydrides of s-block elements. However, there are several groups of superbases that you can look at. For example, amides (diisopropylamide related) are commonly used superbases. More modern are phosphazene bases which are neutral rather bulky compounds containing phosphorus and nitrogen. An interesting topic is a “proton sponge” (or Alder's base) and its derivatives as well as several theoretical and practical approaches used in rational design of superbases.

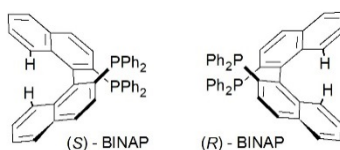
## Chapter 6 An Introduction to Coordination Compounds

- T6.2** The most important part of this problem is deciding on the composition of inner-sphere and outer-sphere complexes of the two compounds mentioned (see *The language of coordination chemistry*). For example, the fact that three equivalents of AgCl can be quickly obtained from a solution of the pink salt indicates that three  $\text{Cl}^-$  anions are a part of the outer-sphere complex. The rest, combined together, should form the inner-sphere complex  $[\text{Co}(\text{NH}_3)_5(\text{OH}_2)]^{3+}$ , and the salt should be  $[\text{Co}(\text{NH}_3)_5(\text{OH}_2)]\text{Cl}_3$ . It can be demonstrated similarly that the purple solid is  $[\text{CoCl}(\text{NH}_3)_5]\text{Cl}$ . These guidelines are useful for Tutorial Problems 7.3 and 7.5 as well.
- T6.4** The vital part of information for determining the structure (and hence the name) of the diaqua complex is the fact that it does not form a chelate with (otherwise chelating) 1,2-diaminoethane ligand, not so much the fact that we have started with *trans* isomer. Consult Figure 6.4 in your textbook to determine the structure of the diaqua complex. For the third isomer you have been given an *empirical* composition of  $\text{PtCl}_2 \cdot 2\text{NH}_3$ . The actual composition can have any multiple of 1 : 2 ratio (i.e., the actual composition might be  $2\text{PtCl}_2 \cdot 4\text{NH}_3$ , or  $3\text{PtCl}_2 \cdot 6\text{NH}_3$ , etc. as long as the simplest ratio remains 1 : 2). If you look at the products from the reaction with  $\text{AgNO}_3$ , you will see that one contains a cation  $[\text{Pt}(\text{NH}_4)_4]^{2+}$  and the other anion  $[\text{PtCl}_4]^{2-}$  as inner sphere complexes. Simply combining the two we have the third isomer  $[\text{Pt}(\text{NH}_4)_4][\text{PtCl}_4]$  with composition  $2\text{PtCl}_2 \cdot 4\text{NH}_3$ . (This is the special case isomerism sometimes referred to as polymer isomerism because the isomers differ by the number of empirical formula units, or monomers, in their structure; for example, in this case the general formula of the polymer isomers can be written as  $(\text{PtCl}_2 \cdot 2\text{NH}_3)_n$  with  $n = 2$ .) The name for the third isomer is tetraammineplatinum(II) tetrachloridoplatinate(II).
- T6.9** Recall from other courses that amines with three different substituents on N atom should be chiral, but due to the fast isomerization this chirality is not observed in real situations. Once, however, the N atom coordinates

to the metal, the isomerization is not possible any longer—in this case particularly because the N atoms become a part of a rigid chelating ring.



- T6.11** BINAP (short for (2,2'-bis(diphenylphosphino)-1,1'-binaphthyl)) has axial chirality with the chiral axis coinciding with the C–C bond connecting two naphthyl systems. The bulky diphenylphosphino groups as well as indicated H atoms on naphthyl groups prevent the rotation around this C–C bond making the structure stable with respect to racemisation:

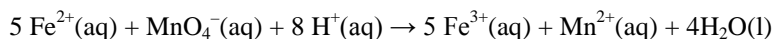


Combine this chirality of BINAP ligand with what you learned about the chirality of complexes to discuss the chirality of BINAP-containing complexes.

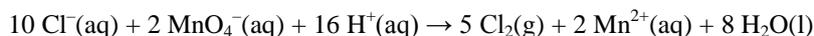
- T6.12** The relevant sections are 6.13 and 6.14, trends in successive formation constants and chelating effect.
- T6.13** Rotaxanes are molecular machines—a very interesting research topic since the Nobel prize in chemistry for 2017 was awarded to the three scientists pioneering the concept and syntheses of rotaxanes: Jean-Pierre Sauvage, Sir J. Fraser Stoddart and Bernard L. Feringa. Their work is a good starting point for discussion. Pseudorotaxanes are intermediates in the rotaxane synthesis. The material relevant to coordination chemistry in their synthesis is found in Box 6.4.

## Chapter 7 Oxidation and Reduction

- T7.1** The reaction for analytical determination of  $\text{Fe}^{2+}$  with  $\text{MnO}_4^-$  is:



with  $E^\circ = E^\circ_{\text{red}} - E^\circ_{\text{ox}} = +1.51 \text{ V} - (+0.77\text{V}) = +0.74\text{V}$ . If HCl is present, the following side-reaction can take place:



with  $E^\circ = E^\circ_{\text{red}} - E^\circ_{\text{ox}} = +1.51 \text{ V} - (+1.36\text{V}) = +0.15\text{V}$ . From  $E^\circ$  values it is clear that oxidation of  $\text{Fe}^{2+}(\text{aq})$  is more favourable under the standard conditions than oxidation of  $\text{Cl}^-(\text{aq})$  because  $E^\circ(1) > E^\circ(2)$ . However, as reaction (1) is reaching equilibrium its potential difference is changing according to equation:

$$E = E^\circ - \frac{RT}{\nu F} \ln \frac{[\text{Fe}^{3+}]^5 [\text{Mn}^{2+}]}{[\text{Fe}^{2+}]^5 [\text{MnO}_4^-] [\text{H}^+]^8}$$

As  $[\text{Fe}^{3+}]$  and  $[\text{Mn}^{2+}]$  are increasing, so is  $Q$ , and  $E$  decreases. At one point the two potentials are going to invert, that is,  $E(1) < E(2)$  and reaction (2) is going to be more favourable. To avoid the side reaction we have to keep  $E(1) > E(2)$ . If the phosphate anion stabilizes  $\text{Fe}^{3+}$ , that means that through complexation we can make the  $\text{Fe}^{3+}/\text{Fe}^{2+}$  potential more negative, meaning that  $E(1)$  becomes more positive and reaction (1) more favourable (see Section 7.10 *The influence of complexation*). Addition of  $\text{Mn}^{2+}$  would influence both reactions but more on reaction (2) than (1) because 2 equivalents of  $\text{Mn}^{2+}$  are produced in (2) while only one in (1). You can see this effect if you write down reaction quotients for both (1) (given above already) and (2).

- T7.2** Keep in mind that the standard reduction potentials can provide not only information about spontaneity of a given reaction in aqueous solutions, but also provide an insight if side reactions are going to take place: Could

water be oxidized or reduced? Can a species be oxidized with atmospheric oxygen? How will the reaction direction change with pH etc. It is good idea to at least mention Pourbaix diagrams and their use in inorganic environmental chemistry and geochemistry (speciation chemical species, their mobility, etc.) as well as point to the problems of corrosion in aqueous media and how reduction potential can be used to both predict the possibility of corrosion and protect from it.

- T7.3** If you have problems with this project, review Section 7.3 *Trends in standard potentials*.
- T7.4** Review Section 7.10 *The influence of complexation* to work on this project. You have been given a hint for the value for [Fe(II)(Ent)] stability constant, and you may consult Resource Section 3 for the standard reduction potential for Fe<sup>3+</sup>/Fe<sup>2+</sup> couple. Also note the pH conditions for this reduction.

## Chapter 8 Physical Techniques in Inorganic Chemistry

- T8.2** Review Section 8.2 of the main text.
- T8.3** You must think about two important factors when considering hydrogen storage materials. First, the candidates for hydrogen storage materials are based on both compounds containing light elements (most notably B and N) and transition metals. These two groups can require different methods of analysis. Second, ultimately the good hydrogen storage material should “pack” a lot of hydrogen (a good measure of this is the weight percentage of H stored in the material—you do not want to carry around a lot of weight that contains very little useful material), and the analysis of hydrogen content itself presents some challenges.
- T8.5** Hydrogen bonding usually results in the broadening of O-H stretching frequencies. A very good text for the IR in general is Nakamoto’s book provided in the “Further Reading” section of this chapter.
- T8.9** Some suggestions (with details on *how* in the chapter): a) and b) atomic absorption or emission spectroscopy, c) IR (BrF<sub>5</sub> is a liquid so X-ray diffraction at room temperature is not possible), d) X-ray diffraction on a single crystal, e) NH percentage analysis could be helpful
- T8.10-12** Any analytical chemistry textbook will describe the analysis of the data collected using AAS. Form your “Further Reading” list Skoog’s text is a good reference point.

## Chapter 9 Periodic Trends

- T9.1** Follow the logic outlined by the section of this chapter. For each property extrapolate from known values to get the prediction for the new elements.
- T9.5** A good starting reference for this exploration is Eric R. Scerri. (1998). “The Evolution of the Periodic System.” *Scientific American*, 279, 78–83 and references provided at the end of this article. The website “The Internet Database of Periodic Tables” ([http://www.meta-synthesis.com/webbook/35\\_pt/pt\\_database.php](http://www.meta-synthesis.com/webbook/35_pt/pt_database.php)) is also useful. From the modern designs (post-Mendeleev), interesting ones to consider are Hinrichs’ spiral periodic table, Benfey’s oval table, Janet’s left-step periodic table, and Dufour’s tree.

## Chapter 10 Hydrogen

No guidance available

## Chapter 11 The Group 1 Elements

- T11.7** Sodide ion is not produced by simply dissolving Na in NH<sub>3</sub>(l). See section 11.14 *Solutions in Liquid Ammonia* for details. Dissolved Na produces Na<sup>+</sup> in ammonia. This cation will not be involved in hydrogen bonding because hydrogen in NH<sub>3</sub> is delta-positive. Na<sup>+</sup> is going to interact with lone electron pair on NH<sub>3</sub> molecule.

## Chapter 12 The Group 2 Elements

- T12.4** BeF<sub>2</sub> is in many ways similar to SiO<sub>2</sub>. A good starting point for the discussion of BeF<sub>2</sub> glasses is structural and chemical similarity between BeF<sub>2</sub> and SiO<sub>2</sub>. A good reading on the topic is Greenwood and Earnshaw (1997) *Chemistry of the Elements*, 2nd ed. Elsevier (Chapter 5).
- T12.7** When discussing these structures, it is useful to consider simple properties, such as ionic radii of Be<sup>2+</sup>, Al<sup>3+</sup>, Si<sup>4+</sup> and P<sup>5+</sup> for coordination number 4. If these are not similar to each other, then there is limited possibility for exchange (i.e., formation of beryllorphosphates). There is an abundance of information on aluminosilicates, including your textbook. For specific minerals, a good starting point is [www.webmineral.com](http://www.webmineral.com) website, a trusted source on mineral data, which can be searched by element. A well-characterized beryllorphosphate mineral is pahasapaite, with zeolite-like framework composed of BeO<sub>4</sub> and PO<sub>4</sub> tetrahedra. This structure is also a good starting point for comparison between beryllorphosphates and aluminosilicates.

## Chapter 13 The Group 13 Elements

- T13.1** The important comparisons are that of charge and ionic radii, consequently the charge density discussion is also relevant. Particularly interesting are biological activities of K<sup>+</sup> and Tl<sup>+</sup> with the difference in biological effect resulting from differences in Lewis acid hardness (soft vs. hard) and tendency to form complexes.
- T13.7** Synthesis of GaN can be achieved using several methods. Simple internet search will provide basic results. The structure is that of wurtzite.

## Chapter 14 The Group 14 Elements

- T14.2** You can use any mineralogy textbook as a source for this problem. Suggested text would be a classic mineralogy textbook *Dana's Manual of Mineralogy* by C. Klein and B. Dutrow, published by Wiley and Sons, currently in its 23rd edition.
- T14.3** The obvious choice for silicon is, of course, the fact that it is in the same group as carbon. They also share the common highest (and most stable) valence and preferred geometry (tetrahedral). The fact that silicon is the second most abundant element in Earth's crust (as well as in crusts of the other rocky planets—at least as much as we know currently) also goes in favour of silicon-based life. The major part of your arguments against should focus on explaining the reasons behind different catenation preferences for the two elements, lack of Si=Si bonds (or better said, their low stability), and silicon's high affinity toward oxygen (the most abundant element in Earth's crust—explain how this is an issue using thermodynamic parameters provided in the tables within this chapter).
- T14.4** The text suggested for T14.2 also discusses the synthetic diamonds and provides further sources on this topic, thus it is a good starting point for this tutorial problem as well.
- T14.10** The structure of Cu<sub>2</sub>ZnSnS<sub>4</sub> has appeared several times in the literature, most recently in Ritscher *et al.* *Journal of Solid State Chemistry* (2016) **238**, p. 68. The structure is tetragonal and can be approximately described as two cubic close packed unit cells composed of S<sup>2-</sup> stacked one on top of each other with metal cations occupying half of tetrahedral holes. The introduction section of this article also contains information and sources relevant to other questions of this tutorial.

## Chapter 15 The Group 15 Elements

- T15.4** Note that traditionally phosphates have been removed from sewage waters by precipitation. Recently, however, new methods have been developed, including biological treatment of waters. Try to analyse the chemical precipitation reactions, look at the metals used and issues related to each (including cost and

potential side-effects). Any textbook covering water treatment and analysis will have both chemical and engineering sides of the process covered.

## Chapter 16 The Group 16 Elements

No guidance available

## Chapter 17 The Group 17 Elements

No guidance available

## Chapter 18 The Group 18 Elements

No guidance available

## Chapter 19 The d-block Elements

**T19.3** Very good overview of both processes can be found in Greenwood, N.N. and Ernschaw, A. (1997). *Chemistry of the Elements*, 2nd ed. Elsevier, in chapter on the Group 4 elements.

**T19.4** After the Earth's atmosphere became oxidizing, the availability of many biologically important elements changed: Fe and N became very difficult to extract whereas Cu became available. For Fe availability, start by considering in which compounds iron occurs in nature frequently. Then compare the solubilities, solution properties, and movability of  $\text{Fe}^{2+}$  and  $\text{Fe}^{3+}$  analogues. Also, look up biologically important compounds known as siderophores. Compare their structures, coordination properties, and stabilities of Fe-siderophore complexes with the man-made chelating reagents such as edta. Pay attention to the process of Fe release from a siderophore.

**T19.7** A good starting point for this tutorial assignment is the text Schmid, G. (ed.). (2010). *Nanoparticles: From Theory to Application*, 2nd ed. Wiley-VCH. The text gives a general overview of nanoparticles, but has a significant part devoted to gold nanoparticles.

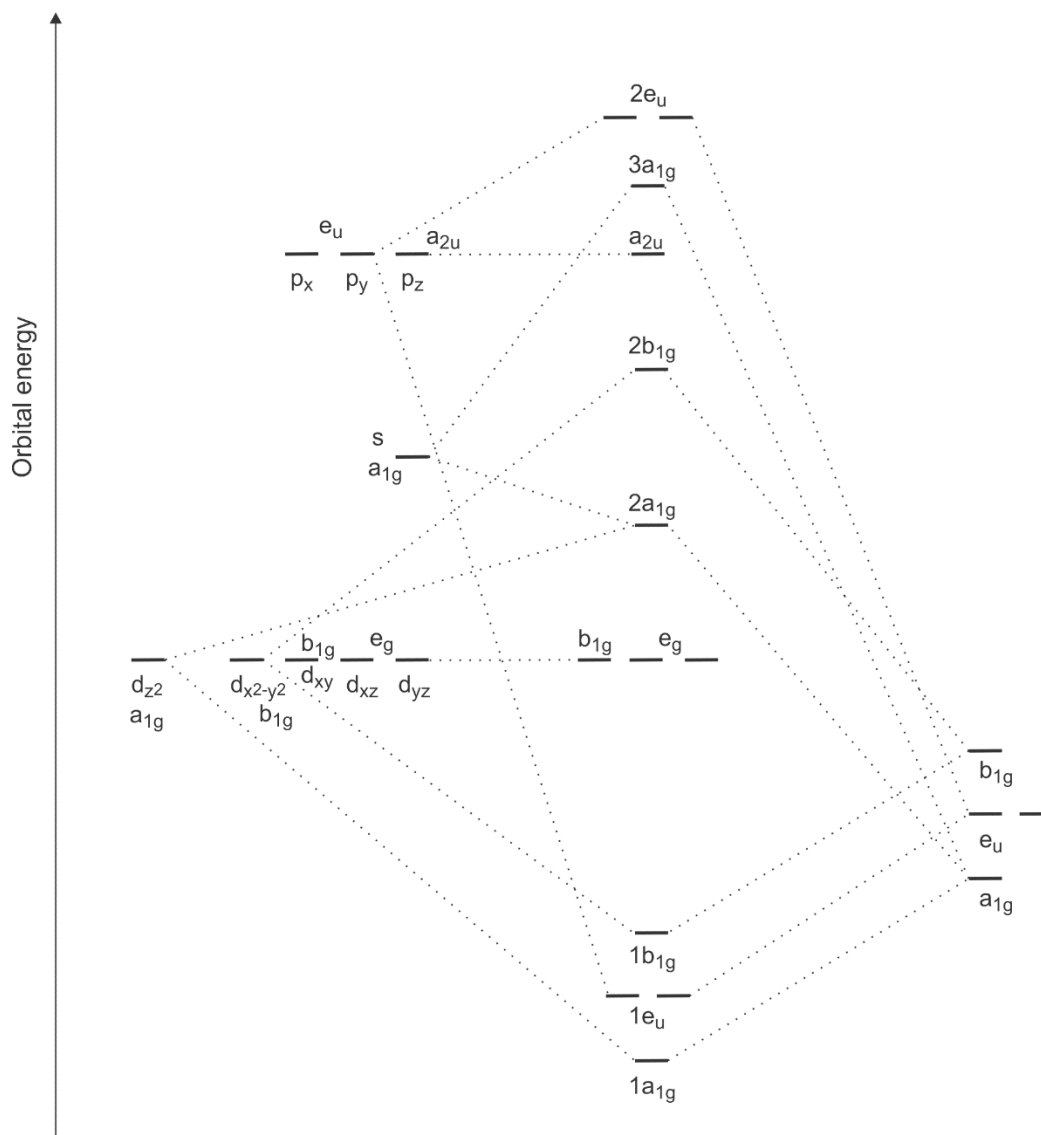
**T19.9** Protiodide was a medical trade name for mercury(I) iodide,  $\text{Hg}_2\text{I}_2$ . Various sources can be used to summarize the side-effects and overdose risks, such as MSDS sheets. Sweetman, S.C. (ed.). *Martindale: The Complete Drug Reference*, published by Pharmaceutical Press, could also be a good source for the toxicity and effects of inorganic mercury salts.

## Chapter 20 d-Metal Complexes: Electronic Structure and Properties

**T20.3** See Problem 20.4 below for guidelines.

**T20.4** From Table RS5.1 in Resource Section 5 we can see how metal orbitals transform in  $D_{4h}$  point group. Thus,  $d_{z^2}$  and s orbitals transform as  $A_{1g}$ ,  $d_{yz}$  and  $d_{xz}$  as  $E_g$ ,  $d_{xy}$  as  $B_{2g}$ ,  $d_{x^2-y^2}$  as  $B_{1g}$ ,  $p_z$  as  $A_{2u}$ , and finally  $p_x$  and  $p_y$  as  $E_u$ . Looking in  $D_{4h}$  column we can also find ligand orbitals: singly degenerate  $A_{1g}$  and  $B_{1g}$  and doubly degenerate  $E_u$ . These are the only possible ligand symmetry adapted linear combinations that are relevant for purely  $\sigma$  bonding. The molecular orbital diagram is shown on the next page. Note that the metallic  $d_{xy}$ ,  $d_{xz}$ ,  $d_{yz}$ , and  $p_z$  atomic orbitals have no symmetry match on ligand side and they remain non-bonding in a pure  $\sigma$  bonding scenario. These orbitals do have a match if we include  $\pi$  bonding. Analysis of  $D_{4h}$  column for ligand SALC reveals a singly degenerate  $A_{2u}$  set (a match for  $p_z$  metallic orbital) and a doubly degenerate  $E_g$  set (a match for  $d_{xz}$  and  $d_{yz}$ ). With inclusion of  $p$  bonding, only  $d_{xy}$  (of  $B_{2g}$  class) remains non-bonding. Note that this diagram can serve as a basis for tutorial Problem 20.3 as well. *Trans*- $[\text{ML}_4\text{X}_2]$  complex also has a  $D_{4h}$  symmetry, so the metal orbital classes remain the same. It can be derived from square planar  $\text{ML}_4$  (for which the diagram applies) by adding two X ligands along z axis. Thus, what we have to add on the ligand side of the molecular orbital diagram is a singly degenerate  $A_1$  set that is a good match for both  $d_{z^2}$  and s

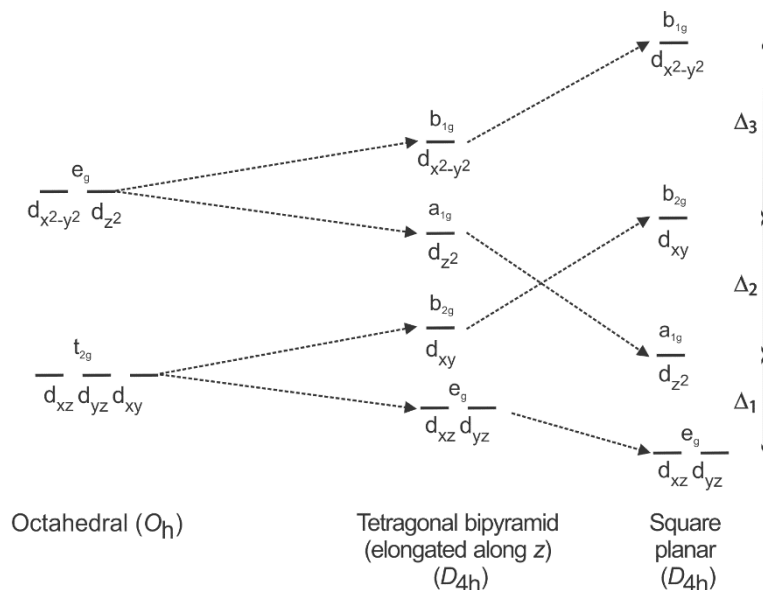
metallic orbitals. The new ligand orbitals should be *higher* in energy than the ones shown in the figure below because X is lower than L in the electrochemical series..



**T20.5** The figure below shows the rough orbital diagrams indicating changes in energy as we go from an octahedral complex ( $O_h$ ) to a tetragonally distorted ( $D_{4h}$ ) to finally square planar one when the ligands along  $z$  axis have been completely removed. If we elongate the bonds along  $z$  axis, the repulsion between ligands (as point charges) and electrons in all  $d$  orbitals that have  $z$  component ( $d_{z^2}$ ,  $d_{xz}$ , and  $d_{yz}$ ) is going to decrease. Therefore, these  $d$ -metallic orbitals are going to drop in energy in a tetragonally distorted complex and will break the degeneracy of  $t_{2g}$  and  $e_g$  sets (the Jahn-Teller theorem). The ligands along  $x$  and  $y$  axes now can approach metal a bit closer (due to less steric crowding), will repel the electrons in  $d_{x^2-y^2}$  and  $d_{xy}$  more than in  $O_h$  symmetry, and will consequently increase in energy in comparison to starting octahedral complex. Square planar geometry results when we completely remove the ligands along  $z$  axis. In this case the ligands are approaching the metal centre along  $x$  and  $y$  axes and strongly repel with the electrons in  $d_{x^2-y^2}$  orbital (remember that this orbital has its lobes located exactly along  $x$  and  $y$  axes). The energy of this orbital increases significantly. The energy of  $d_{xy}$  orbital is also increasing because its lobes are between  $x$  and  $y$  axes. All orbitals that have  $z$  axis component decrease in energy because the point charges have been removed along this axis. Note, however, that the energy of  $d_{z^2}$  orbital is not the lowest one, as we might expect. This is because  $d_{z^2}$  orbital has some electron density in  $xy$  plane in a torus shape.

Similar analysis can be applied to derive  $d$  orbital splitting for linear two coordinate complexes if we, starting from the octahedral complex, remove ligands along  $x$  and  $y$  axes. In this case we can consider a squished octahedron as an intermediate geometry (with axial  $M-L$  bonds shorter than equatorial  $M-L$  bonds). Your

result should have  $d_{z^2}$  as the orbital of highest energy, followed by doubly degenerate  $d_{xz}$  and  $d_{yz}$ , and finally lowest in energy is another doubly degenerate set of  $d_{xy}$  and  $d_{x^2-y^2}$ .



## Chapter 21 Coordination Chemistry: Reactions of Complexes

- T21.3** The data in the table is related to the Figure 21.1 and Table 21.1 in the main text. All values should be discussed in the context of this section except for  $[\text{Cr}(\text{H}_2\text{O})_5(\text{OH})]^{2+}$ .
- T21.2** As  $\text{PET}_3$  is added, an exchange between coordinated and free  $\text{PET}_3$  would affect the shape of the hydride signal. Once a large excess of  $\text{PET}_3$  is added it is likely that a pentacoordinate complex  $[\text{Pt}(\text{H})(\text{PET}_3)_4]^+$  is formed. If this complex is fluxional, then rapid Berry pseudorotation can make any coupling between hydride and phosphorus atom unobservable.

## Chapter 22 d-Metal Organometallic Chemistry

No guidance available

## Chapter 23 The f-Block Metals

- T23.6** It would be a good idea (and practice as well) not only to compare the Latimer diagrams provided in the Resource Section 3, but also to construct one Frost diagram with data for both Np and Re to compare the two elements directly. Also note which oxidation states are missing for Re and Np and the chemical composition of the species for each oxidation state of the elements—this gives you a more complete idea of the differences between the two elements.
- T23.8** Consult Greenwood, N.N., Earnshaw, A. (1997). *Chemistry of the Elements*, 2nd ed. Elsevier (pp. 1260–1262), and references therein. Also, a good source is Morss, L. R., Edelstein, N. M., Fuger, J. (eds.). (2006). *Chemistry of the Actinide and Transactinide Elements*, Vol. 2. Dordrecht, NLD: Springer.

## Chapter 24 Materials Chemistry and Nanochemistry

- T24.1** One of the most popular lambda sensors contains zirconia ( $\text{ZrO}_2$ ) as a solid electrolyte. This material has a high conductivity for  $\text{O}^{2-}$  ions at elevated temperatures. The cell responds to the changes in  $\text{O}_2$  partial pressure in exhaust gas. The reduction potential for  $\text{O}_2(\text{g}) + 4\text{e}^- \rightarrow 2\text{O}^{2-}(\text{s})$  is proportional to  $p(\text{O}_2, \text{reference})/p(\text{O}_2, \text{exhaust gas})$ , with partial pressure of  $\text{O}_2$  in the air as the reference. (See Section 24.4(b) *Solid anionic electrolytes* and refer to Figure 24.9).
- T24.3** Recall from Section 24.8(a) *Nitrides* that heating complex oxides under stream of ammonia can lead to the partial reduction of metal oxide. It can also lead to the nitridation of the oxide forming oxide-nitrides and eventually, with high excesses of ammonia, nitrides. In this case, partial nitridation occurs:  
$$2\text{SrWO}_4 + 2\text{NH}_3 \rightarrow \text{Sr}_2\text{W}_2\text{O}_5\text{N}_2 + 3\text{H}_2\text{O}.$$
 $\text{Sr}_2\text{W}_2\text{O}_5\text{N}_2$  adopts the pyrochlore structure.
- T24.5** Delafossite is a mineral with chemical composition  $\text{CuFeO}_2$ . Its structure has been described in Pabst, A. (1938) *American Mineralogist*, **23**, 175–176, and more recently revisited (with a look at electronic properties of this material) in Marquardt, M., Ashmore, N., & Cann, D. (2006). *Thin Solid Films*, **496**(1), 146–156. Connect this research with the fact that  $\text{Fe}_2\text{O}_3$  can also be used as a photocatalyst, as mentioned in Section 24.18 *Photocatalysts*.
- T24.7** The earliest reports of a superconducting material based on  $\text{LnFeOAs}$  structure were Kamihara, Y. et al. (2008). *J. Am. Chem. Soc.* **130**, 3296, and Takahashi, H. et al. (2008). *Nature* **453**, 376, both reporting the structure and superconducting properties of  $\text{La}[\text{O}_{1-x}\text{F}_x]\text{FeAs}$ . Sm, Ce, Nd, Gd, and Pr analogues were all reported in the same year as well. Some useful references are: Chen, X. H. et al. (2008). *Nature* **354**, 761 (for Sm), Chen, G. F. et al. (2008). *Phys. Rev. Lett.* (Ce analogue); Ren, Z. A. et al. (2008). *Europhysics Lett.* **82**, 57002, (Nd analogue); Ren, Z. A. et al. (2008). arXiv:0803.4283. (Pd analogue). These are historically interesting, and you should look up more current sources as well.
- T24.9** Two relatively recent sources are useful: Hischer, M. (ed.). (2010). *Hydrogen Storage: New Materials for Future Energy Storage*. Hoboken: John Wiley & Sons, Incorporated; and Godula-Jopek, A. et al. (2012). *Hydrogen Storage Technologies: New Materials, Transport, and Infrastructure*. Weinheim: Wiley-VCH.
- T24.11** A very good starting point for this research is Guo, J., Chen, X. (2012). *Solar Hydrogen Generation: Transition Metal Oxides in Water Photoelectrolysis*. New York: McGraw-Hill Professional.

## Chapter 25 Biological Inorganic Chemistry

- T25.2** Consider what is meant by the term “efficiency” in catalysis. In terms of mechanistic questions, consider the complexity of the process for production of  $\text{NH}_3$  from  $\text{N}_2$  as well as the complexity of the nitrogenase cofactor. For example, can the 3D structure help to decide on the binding site of  $\text{N}_2$ ? Does it reveal much about the electron flow within the cofactor? What happens to a produced  $\text{NH}_3$  molecule (how is it removed from the active site)? Consider also the details about the active site structure we are missing.

## Chapter 26 Inorganic Chemistry in Medicine

- T26.2** Some useful sources (and references cited within) are:
- I. Bratsos, T. Gianferrara, E. Alessio, C. G. Hartinger, M. A. Jakupec, and B. K. Keppler. (2011). Chapter 5: Ruthenium and other non-platinum anticancer compounds. In Alessio, E. (ed.), *Bioinorganic Medicinal Chemistry*. Weinheim: Wiley-VCH Verlag & Co.
- G. Gasser, I. Ott, N. Metzler-Nolte. (2011). Organometallic anticancer compounds. *Journal of Medicinal Chemistry* **54**(1), 3–25.
- C. G. Hartinger, P. J. Dyson. (2009). Bioorganometallic chemistry—from teaching paradigms to medicinal applications. *Chemical Society Reviews* **38**(2), 391–401.